

# Structural and Microhardness Changes After Turning of the AISI 1045 Steel for Minimum Quantity Cooling Lubrication

Radosław W. Maruda, Grzegorz M. Krolczyk, Mariusz Michalski, Piotr Nieslony, and Szymon Wojciechowski

(Submitted July 7, 2016; in revised form October 30, 2016; published online November 30, 2016)

This work presents the cooling effect under minimum quantity cooling lubrication and dry cutting on structural changes and microhardness of the ferritic-pearlitic AISI 1045 steel after turning. Due to the fact that the AISI 1045 steel has a two-phase structure, microhardness tests using the Vickers method were conducted with a load of 0.05 HV separately for ferrite and pearlite grains. The tests showed that cooling of the cutting zone under minimum quantity cooling lubrication (MQCL) condition decreased the depth of the hardened layer compared to dry cutting by approximately 40% for both pearlite and ferrite. Scanning electron microscopy analysis revealed that applying MQCL limits the formation of plastic deformations, among others, by reducing the surface crumple zone by approximately 50% compared to dry cutting. As a result of cooling being applied to the cutting zone using the MQCL method, the average diameter of ferrite grains has been decreased in the entire surface area compared to dry cutting. When using dry cutting, clear structural changes of the surface layer were also observed. This may be the result of sulfide inclusions which have formed, causing microcracks on the edge of the hardened layer and surface deformation visible as notches.

**Keywords** AISI 1045, dry cutting, microhardness, MQCL, SEM analysis, surface integrity, turning

## 1. Introduction

Cutting methods significantly affect work efficiency and also considerably affect surface integrity (SI) of the workpiece. These changes are caused by high temperatures in the cutting zone which result in plastic deformation (residual stresses), chemical reactions taking place in the chip-tool interface and changes in the surface layer (microcracks, roughness) (Ref 1). The surface of the workpiece after machining is usually resistant to the effect of most stresses occurring during the machining process as well as the effect of many different environmental factors (Ref 2). However, improperly chosen cutting conditions may lead to reduced efficiency of production. Generally, stresses are influenced by two factors: plastic deformation and changes in the volume of material related to temperature and metallurgic changes in the structure (Ref 3, 4).

Research concerning the influence of the method of cooling the cutting zone during turning on creating SI is a very important issue, since SI analyzes the condition of the surface layer and its influence on functional and mechanical properties

of the machined material (Ref 2). The most important features of SI are: roughness, microhardness, depth of the surface layer, topography of the surface and chemical composition of the workpiece (Ref 5). Industrial metrology is a broad field of science, and its proper application allows to obtain quality products (Ref 6-9).

Metalworking fluids (MWFs) play an important role in machining. Proper choice of MWFs not only increases the accuracy and quality of the machined surface (Ref 10), but also reduces friction in the tool-workpiece contact area (Ref 11), as well as prevents excessive heat generation by cooling the cutting area (Ref 12). Flood cooling is the most common cooling method. However, due to social, economic and environmental aspects, research concerning green manufacturing, which is a part of green engineering, is currently ongoing. The purpose of green engineering is to design and utilize production processes which are economical and at the same time minimize generation of pollution at the source as well as dangers to human health and the natural environment (Ref 13-16).

The best way to reduce the negative effects of MWFs is to completely eliminate them; this is the so-called dry cutting. However, due to tool life and poor surface quality, methods based on minimum quantity lubrication—MQL (Ref 3, 4, 13, 14, 17, 18)—and minimum quantity cooling lubrication—MQCL (Ref 9, 18, 19)—are good alternatives. In both these methods, the amount of active medium in the form of aerosol typically does not exceed 50 ml/h (Ref 4, 18, 20), while for flood cooling method flow rate of MWFs is over the 500 ml/h (Ref 20). In the MQL method, oil is the main active medium (Ref 4, 13, 18); hence, its main purpose is to lubricate, while in the MQCL method an emulsion concentrate is usually the main medium, which is why in this method the primary task is to cool the cutting zone and therefore to dissipate as much heat as possible (Ref 12, 21).

**Radosław W. Maruda** and **Mariusz Michalski**, Faculty of Mechanical Engineering, University of Zielona Góra, 4 Prof. Z. Szafrana Street, 65-516 Zielona Góra, Poland; **Grzegorz M. Krolczyk** and **Piotr Nieslony**, Faculty of Mechanical Engineering, Opole University of Technology, 76 Proszkowska Street, 45-758 Opole, Poland; and **Szymon Wojciechowski**, Faculty of Mechanical Engineering and Management, Poznań University of Technology, 3 Piotrowo Street, 60-965 Poznań, Poland. Contact e-mail: g.krolczyk@po.opole.pl.

Vast studies of environmentally friendly processes confirmed that compared to dry cutting and flood cooling methods, the MQL and MQCL methods reduce tool wear (Ref 3, 17), temperature (Ref 13) and the cutting force (Ref 11, 14); they minimize friction in the tool-workpiece contact area (Ref 11), increase surface quality (Ref 4, 10, 14) and positively affect chip formation zone (Ref 18).

Krolczyk et al. (Ref 22) proved that microhardness tests of a two-phase stainless steel are necessary in order to better analyze processes in the surface layer. They found that lubricated turning of austenitic-ferritic stainless steel caused a decrease in depth of hardened layer approximately about 40% compared to dry cutting.

Hassanpour et al. (Ref 23) found that when MQL method is used, out of all four cutting parameters, feed rate had the greatest influence on microhardness during milling of the AISI 4340 steel, while cutting speed had the greatest influence on thickness of white layer.

Gao et al. (Ref 24) presented considering the process of continuous induction hardening of the AISI 1045 steel, separate tests of each of the steel's phases for microhardness, stresses and analysis of the microstructure are necessary.

Pu et al. (Ref 25) studied effect of changes in the microstructure of the AISI 1045 steel in the tool-workpiece contact zone on the diffusion wear depending on the variable cutting speed during the turning. Studies have shown that the largest changes in the structure occur above 367 m/min due to dynamic recrystallization. The images obtained by field-emission scanning electron microscopy showed that with the increase in the cutting speed grain size of different phases also increased.

The purpose of this work is to present the effect of cooling conditions of the cutting zone using the MQCL method during

the process of turning on microhardness of the AISI 1045 steel. Special attention was paid to deformation of the surface layer and sulfide inclusions forming in dry cutting as well as changes in thickness of the hardened layer depending on the method of cooling.

## 2. Experimental Materials and Procedures

The material used in the experiment was AISI 1045 carbon steel. Its chemical composition, mechanical properties and structure are presented in Table 1. It can be seen that the AISI 1045 steel is a two-phase material composed of pearlite (darker) and ferrite (brighter).

Six percentage EMULGOL-S, an emulsion concentrate based on mineral oil and 94% water, was the active medium in the MQCL method; it was prepared using an electromagnetic stirrer, type ES21H. Lenox 1LN micronizer (Fig. 1), with the ability to adjust the emulsion flow ( $E = 1.4 \text{ } 100 \text{ g/h}$ ) and the air flow ( $1.2\text{--}5.8 \text{ l/min}$ ), was the device used to form the emulsion mist (Ref 20). The micronizer has three nozzles whose diameter changes with the air flow rate. Air and oil are supplied to the nozzles via separate ducts. The rate of the air flow is much higher than that of the emulsion flow, which causes the emulsion to break into small droplets at the nozzle outlet. For each of the cooling methods, three samples were prepared. Parameters of cutting and emulsion mist formation applied during the experiment are based on the industry recommendations and conclusions from the earlier investigations (Ref 20, 22) and presented in Table 2.

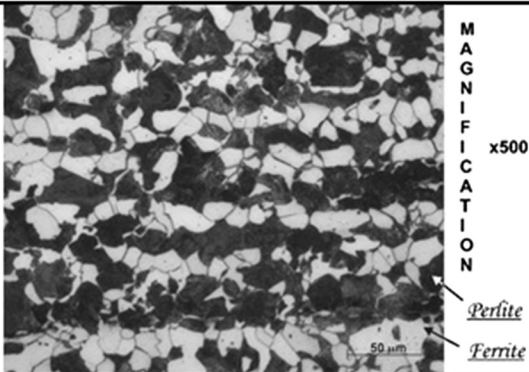
Microhardness was measured using the Zwick ZHV 10 hardness tester. A Paar MHT-4 Vickers indenter with a load of 50 g during 10 s for all the measurements was used in the test. The sample for microhardness measurement was prepared by cutting out a quarter (Fig. 2—preparing the sample); then, a metallographic section was made using an automatic grinder polisher. MD-Piano 220, 600 and 1200 disks were used for grinding. Polishing was performed using MD-DAC disks with DiaDuo diamond suspensions with a granulation of 6 and 3  $\mu\text{m}$ . The metallographic sections were etched using a nitric acid solution in ethanol (Nital).

According to Krolczyk et al. (Ref 22) and Gao et al. (Ref 24), the structure of the two-phase AISI 1045 steel requires hardness tests at the microscale separately for ferrite and pearlite grains. Microhardness was measured into the machined material along a line perpendicular to the surface being machined (radially). The first point of microhardness measurement was located at the distance of up to 15  $\mu\text{m}$  from the machined surface. The second measurement point was set at the distance from the profile of 25  $\mu\text{m}$ , and subsequent measurements were performed every 50  $\mu\text{m}$ , until the hardness of the core has been reached.

A visualization of individual phases of the experiment is presented in Fig. 2.

Metallographic tests were performed using a JSM-5600LV scanning electron microscope manufactured by JEOL coupled with an EDS 2000 x-ray microanalyzer manufactured by IXRF. Qualitative analysis of the structure of examined samples was performed on the basis of an image obtained using a secondary electron detector (SEI). For the analysis of structural changes, representative samples have been selected.

**Table 1 Structure, chemical composition and properties of AISI 1045 steel**

STRUCTURE									
									
CHEMICAL COMPOSITION (%)									
C	Fe	Si <sub>max</sub>	S <sub>max</sub>	P <sub>max</sub>	Mn	Cr <sub>max</sub>	Cu <sub>max</sub>	Ni <sub>max</sub>	
0.42 ±0.5	97.11 ±97.5	0.4	0.045	0.045	0.5 ±0.8	0.4	0.3	0.4	
MECHANICAL PROPERTIES									
R <sub>e</sub> (MPa)	R <sub>m</sub> (MPa)	A <sub>5</sub> (%)	HB						
305	580	16	250						

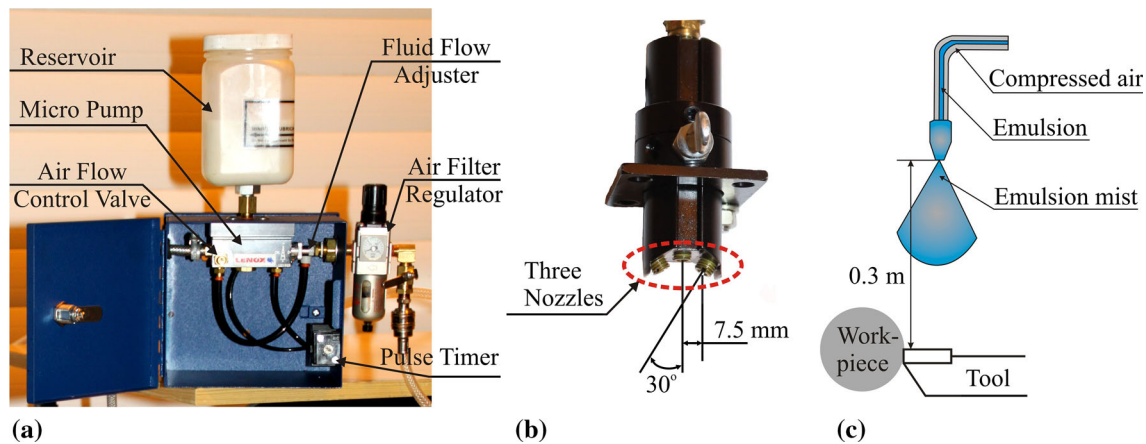


**Fig. 1** Micronizer Lenox 1LN to create emulsion mist: (a) general view; (b) nozzle arrangement; (c) setting of the nozzles in relation to the cutting zone

**Table 2** Experimental conditions

Item	Description
Machine tool	Lathe CNC 400
Cutting tool	TNMG 160408, MM 2025, Ti(C,N)-(2 $\mu$ m) (top layer), Al <sub>2</sub> O <sub>3</sub> -(1.5 $\mu$ m) (middle layer); TiN-(2 $\mu$ m) (bottom layer). Coating technique—CVD
Cutting speed	100 m/min
Feed rate	0.3 mm/rev
Depth of cut	2 mm
Cooling/lubrication condition	Dry cutting MQCL: air pressure: 0.48 MPa, volume air flow: 5.8 l/min, mass flow of active medium: 0.44 g/min, distance between the nozzle and the cutting zone: 0.3 m

### 3. Results and Discussion

#### 3.1 Microhardness Analysis

Surface integrity in cutting processes depends on multiple factors, such as tool geometry, cutting parameters, temperature in the tool-workpiece interface and therefore conditions of the cooling of the cutting zone. Some of the heat generated during the cutting process penetrates into the surface layer of the workpiece and therefore has a considerable effect on the physical parameter of surface integrity, that is, on microhardness. Hence, the method of assessing the effect of means of cooling on microhardness of the AISI 1045 two-phase steel is rationally justified.

Microhardness of the surface layer of the AISI 1045 steel for ferrite and pearlite after the turning is presented in Fig. 3. Obtained values are presented separately for pearlite and ferrite. Pearlite is a stronger strain-hardening phase compared to ferrite.

Obtained values of microhardness in the surface layer (Fig. 3) indicate that the hardness of the surface after dry cutting is greater than that of the surface under MQCL cooling. For top layer under dry cutting, the hardness of pearlite was 419 HV0.05 and the hardness of ferrite was 357 HV0.05, whereas when the MQCL method was used, the hardness of pearlite grains was approximately 342 HV0.05 and the hardness of ferrite grains was 321 HV0.05. When examining the cooling conditions of the cutting zone, it was noticed that cooling using an emulsion mist (MQCL) has a greater effect on decreased hardness of pearlite grains; the difference in hardness between the cooling conditions under consideration in the top layer was

18.3% for pearlite and 10% for ferrite. Under dry cutting condition, it was observed that the hardness of the core was only reached at the depth of 500  $\mu$ m, whereas for the MQCL method it was reached after only 300  $\mu$ m.

The differences between the hardness values in the top layer and in the core can be explained on the basis of three fundamental mechanisms. The first of those is the effect of temperature in the cutting zone for both examined conditions of turning. Intense temperature gradient of the tool-workpiece interface causes phase changes in the workpiece and therefore an increase in hardness. Reactions linked to the environment, such as oxidation or nitrification, which occur on the surface being machined during the cutting process, constitute a second mechanism. Plastic deformations are a third mechanism; they result in changes of the size of the grains and their recrystallization (Ref 26, 27).

#### 3.2 Analysis of the Structural Changes

Tests of the metallographic cross-sections samples of the AISI 1045 steel after dry turning and MQCL method performed using a scanning electron microscope are presented in Fig. 4, along with images after binarization.

Considerable differences in the microstructure of the top layer under applied cutting conditions were observed. In both cases, an occurrence of two zones different from the image of the material's core was noted. Plastically deformed hardened layer forms the first zone, while the coarse-grained structure of steel forms the second. It was found that the hardened layer of the sample subjected to dry turning reaches 14  $\mu$ m into the



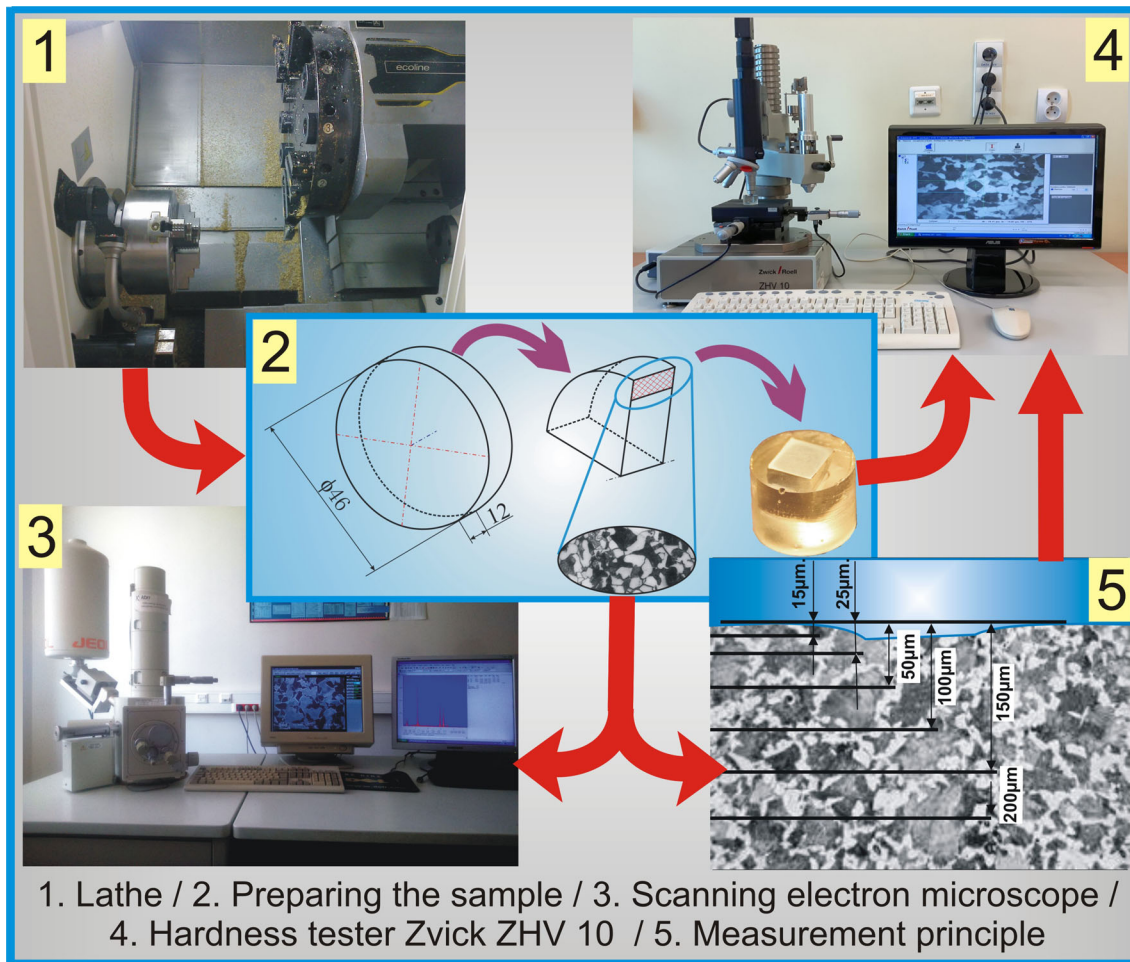


**Fig. 2** Experimental setup

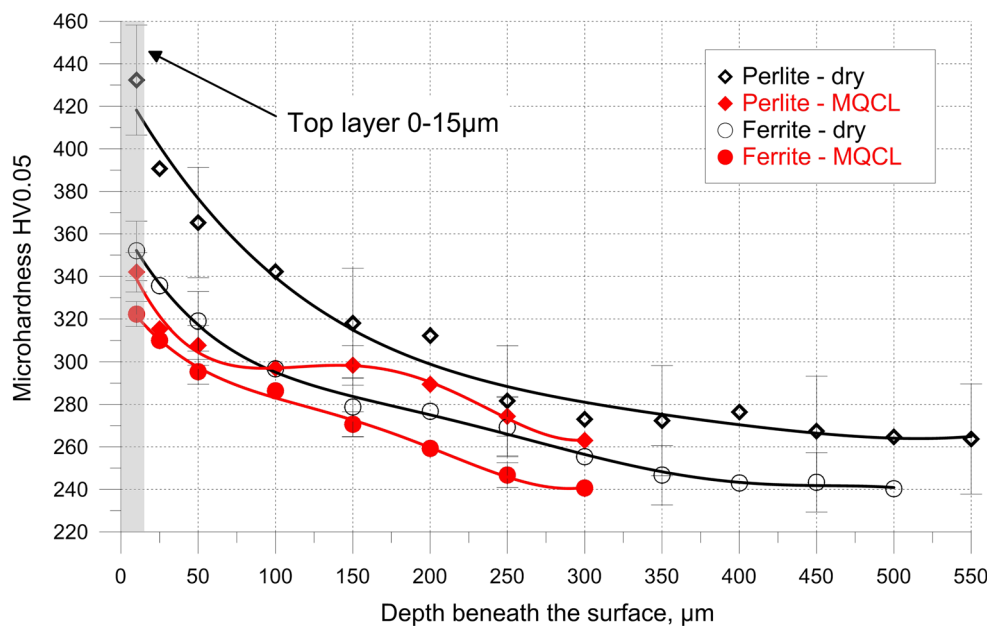


**Fig. 3** Comparison of microhardness depending on method of cooling in the surface layer after the process of turning of the ferritic-pearlitic AISI 1045 steel

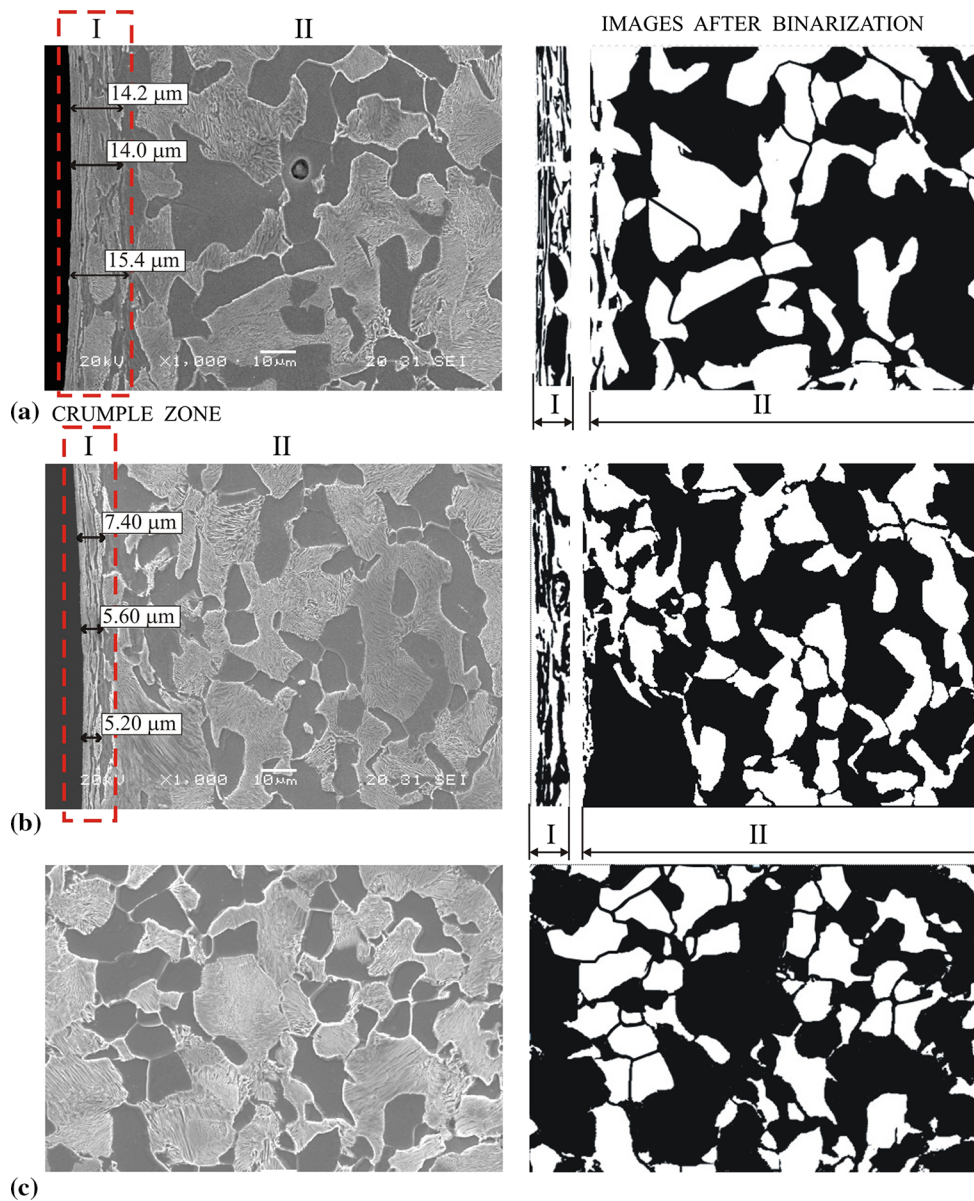


**Fig. 4** Microstructure of the AISI 1045 steel after turning: (a) dry turning—surface layer; (b) MQCL method—surface layer; (c) the core

material (Fig. 4a) and is over twice the size of an analogous zone occurring under cooling with MQCL method (Fig. 4b). The coarse-grained structure of the second zone is particularly visible in the sample subjected to dry turning. In this case (Fig. 4a), pearlite occurs as coarse-grained conglomerates arranged in bands. Pearlite grains in this zone in the second sample subjected to turning under cooling using the MQCL method are also characterized by larger size (Fig. 4b) in relation to the core (Fig. 4c); however, their structure is more dense. A similar situation occurs in case of ferrite located in the second zone, whose grains are much larger and fewer in the sample subjected to dry turning. Greater thickness of the hardened layer in the sample subjected to dry turning, up to 14  $\mu\text{m}$  into the material, is a result of the plasticization of the workpiece due to increased temperature in the cutting zone.

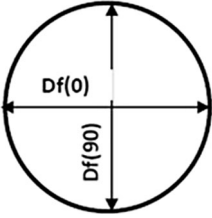
Coarse-grained structure of pearlite and lower amount of ferrite observed in the sample subjected to dry turning confirms

the occurrence of a much higher cutting temperature compared to MQCL.

The average diameter of the ferrite grains for various surface integrity zones depending on the method of cooling is presented in Table 3. Study of images after binarization revealed that the percentage of pearlite and ferrite in the core is equal to 63 and 37%, respectively. Similar ratios were found when assessing the images of zone II for dry turning and turning using MQCL. The ratio of pearlite and ferrite for SI designated as zone II in Fig. 4 has changed; for both methods of cooling, the pearlite/ferrite ratio was found to be 50/50%.

When analyzing the average diameter values of ferrite grains from Table 3, it was found that under cooling using the MQCL method, ferrite grains are approximately 18% smaller in zone II and approximately 32.5% smaller in crumple zone I compared to dry machining.

**Table 3** Average diameter of ferrite grains depending on cooling conditions for the AISI 1045 steel after turning

Measurement of ferrite grains	Zone I		Zone II		Core
	Dry cutting	MQCL	Dry cutting	MQCL	
	2.37	1.44	9.93	7.12	6.69
	9.73	7.17	9.94	9.05	6.95

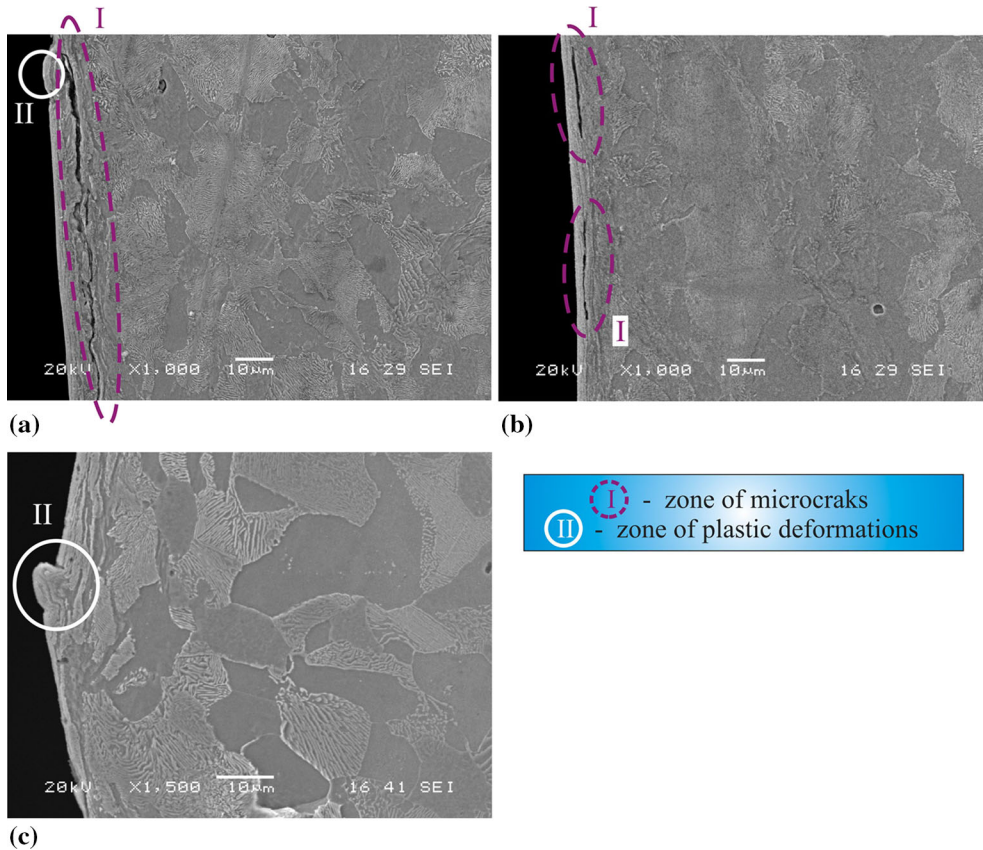


**Fig. 5** Microcracks and deformations in microstructure of the AISI 1045 steel after dry turning (area  $\times 1000$ ): (a) on the edge of the hardened layer, (b) and (c) within the hardened layer

During microscopic examinations, the occurrence of other adverse phenomena in the surface layer of the sample subjected to dry turning, such as cracks, elongated sulfides or notches, was observed. Figure 5(a) presents an example microzone where a crack on the edge between zones 1 and 2 was found. It was also determined that microcracks also occur within the hardened layer (Fig. 5b). This phenomenon may be due to plastic strain of surface layer as a result of the higher temperature in dry cutting process than in MQCL conditions. Nonmetallic inclusions contained in the material are extended (especially sulfide inclusions during hot deformation) and are arranged along the direction of the greatest deformation in a manner reminiscent of the grains.

It was determined that, beyond the formation of a thick hardened layer as well as microfractures, local deformation of the machined surface (Fig. 5a and c) may also occur. Figure 5(c) presents an example effect of this phenomenon—a characteristic notch visible on the cross section of the sample. Over ten such characteristic places were found all along the sample.

Moreover, it was also found that the propagation of microfractures may be caused by sulfides with an adverse, elongated shape (Fig. 6). Such sulfide inclusions can be found on the edge of zones I and II, and their highest concentration was observed under dry cutting.



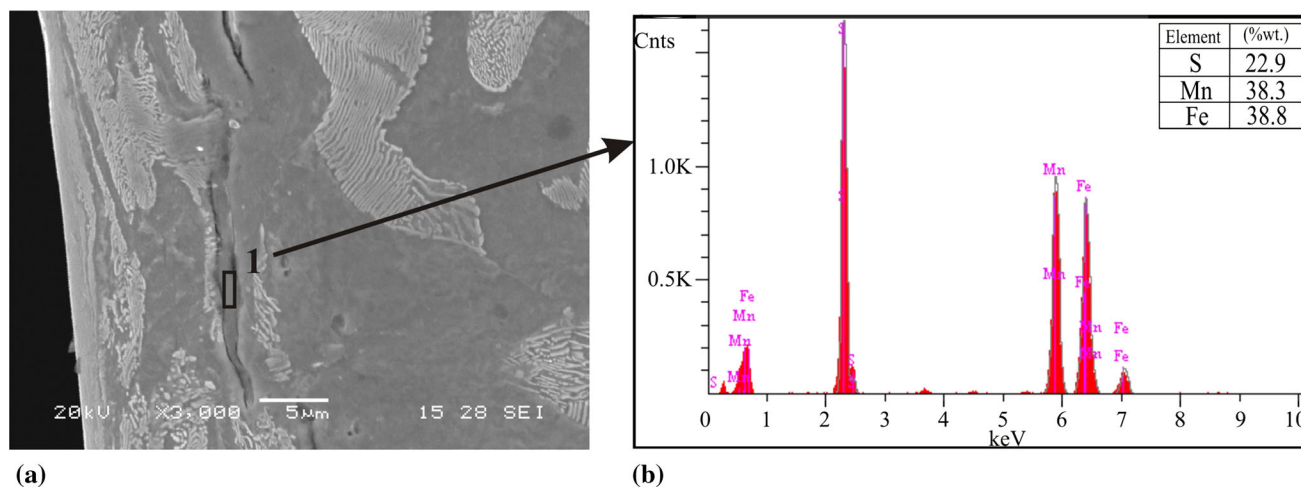


**Fig. 6** Assessment of chemical composition of a sulfide inclusion found in the microstructure of the AISI 1045 steel after dry turning (area  $\times 3000$ ): (a) an image of the structure with the analyzed microzone highlighted, (b) qualitative and quantitative assessment of the chemical composition

## 4. Conclusions

In this research, microhardness and changes in microstructure in the surface layer appearing as microcracks, sulfide inclusions and deformations of the surface of the AISI 1045 steel after turning under various conditions of cooling were compared. Results of the experiment are summarized and presented below:

1. Microhardness distribution on the surface of the sample under cooling using the MQCL method was more uniform compared to dry machining. In the surface layer, microhardness under cooling using an emulsion mist was approximately 10% lower for ferrite and approximately 18.3% lower for pearlite. Using the MQCL method, the depth of the core was reached after only 300  $\mu\text{m}$ , which happened after approximately 500  $\mu\text{m}$  for dry machining.
2. Microstructure analysis showed that under dry machining the crumple zone is twice as big due to plastic deformations compared to cooling using the MQCL method and is equal to 15.4  $\mu\text{m}$  versus 7.4  $\mu\text{m}$ , respectively.
3. Under dry machining, microcracks were found beyond the crumple zone as well as within it. Scanning electron microscopy (SEM) analysis indicates the possibility of sulfide inclusions forming in them.
4. The sample subjected to dry turning showed numerous deformations of the machined surface compared to the sample under cooling using the MQCL method, which confirms the appropriateness of using MQCL to finish machining.
5. Under MQCL cooling, smaller ferrite grains in the entire surface layer were obtained compared to dry machining.

## Open Access

This article is distributed under the terms of the Creative Commons Attribution 4.0 International License (<http://creativecommons.org/licenses/by/4.0/>), which permits unrestricted use, distribution, and reproduction in any medium, pro-

vided you give appropriate credit to the original author(s) and the source, provide a link to the Creative Commons license, and indicate if changes were made.

## References

1. N. Masmiahi, A.A.D. Sarhan, M.A.N. Hassan, and M. Hamdi, Optimization of Cutting Conditions for Minimum Residual Stress, Cutting Force and Surface Roughness in End Milling of S50C Medium Carbon Steel, *Measurement*, 2016, **86**, p 253–265
2. J.P. Davim, *Surface Integrity in Machining*, Springer, Berlin, 2010
3. Y.S. Liao and H.M. Lin, Mechanism of Minimum Quantity Lubrication in High-Speed Milling of Hardened Steel, *Int. J. Mach. Tools Manuf.*, 2007, **47**, p 1660–1666
4. T. Leppert, Effect of Cooling and Lubrication Conditions on Surface Topography and Turning Process of C45 Steel, *Int. J. Mach. Tools Manuf.*, 2011, **51**(2), p 120–126
5. A.M. Abrao, J.L.S. Ribeiro, and J.P. Davim, *Surface Integrity, Machining of Hard Materials*, Springer, Berlin, 2011, p 115–141
6. R. Kumar, S. Chattopadhyaya, A.R. Dixit, B. Bora, M. Zelenak, J. Foldyna, S. Hloch, P. Hlavacek, J. Scucka, J. Klich, L. Sitek, and P. Vilaca, Surface Integrity Analysis of Abrasive Water Jet-Cut Surfaces of Friction Stir Welded Joints, *Int. J. Adv. Manuf. Technol.*, 2016, doi: [10.1007/s00170-016-8776-0](https://doi.org/10.1007/s00170-016-8776-0)
7. W. Kaplonek, K. Nadolny, and W. Habrat, Morphology of Near- and Semispherical Melted Chips After the Grinding Processes Using Sol-Gel Abrasives Based on SEM-Imaging and Analysis. *Adv. Mater. Sci. Eng.*, 2016, doi: [10.1155/2016/2573920](https://doi.org/10.1155/2016/2573920)
8. A. Glowacz and Z. Glowacz, Diagnostics of Stator Faults of the Single-Phase Induction Motor Using Thermal Images, MoAsoS and Selected Classifiers, *Measurement*, 2016, **93**, p 86–93
9. M. Merola, A. Ruggiero, J.S. De Mattia, and S. Affatato, On the Tribological Behavior of Retrieved Hip Femoral Heads Affected by Metallic Debris. A Comparative Investigation by Stylus and Optical Profilometer for a New Roughness Measurement Protocol, *Measurement*, 2016, **90**, p 365–371
10. R.W. Maruda, S. Legutko, G.M. Krolczyk, S. Hloch, and M. Michalski, An Influence of Active Additives on the Formation of Selected Indicators of the Condition of the X10CrNi18-8 Stainless Steel Surface Layer in MQCL Conditions, *Int. J. Surf. Sci. Eng.*, 2015, **9**(5), p 452–465
11. D. Setti, M.K. Sinha, S. Ghosh, and P.V. Rao, Performance Evaluation of Ti-6Al-4V Grinding Using Chip Formation, and Coefficient of Friction Under the Influence of Nanofluids, *Int. J. Mach. Tools Manuf.*, 2015, **88**, p 237–248

12. E. Feldshtein and R. Maruda, Some Regularities of the Heat Transfer in the Process of Cooling of a Cutting Zone by an Emulsion Fog, *J. Eng. Phys. Thermophys.*, 2006, **79**(3), p 606–610
13. M. Hadad and A. Sharbati, Thermal Aspects of Environmentally Friendly-MQL Grinding Process, *Proced. CIRP*, 2016, **40**, p 509–515
14. T. Tawakoli, M.J. Hadad, and M.H. Sadeghi, Investigation on Minimum Quantity Lubricant-MQL Grinding of 100Cr6 Hardened Steel Using Different Abrasive and Coolant-Lubricant Types, *Int. J. Mach. Tools Manuf.*, 2010, **50**, p 698–708
15. F. Pusavec, J. Kenda, and J. Kopac, The Transition to a Clean, Dry, and Energy Efficient Polishing Process: An Innovative Upgrade of Abrasive Flow Machining for Simultaneous Generation of Micro-Geometry and Polishing in the Tooling Industry, *J. Clean. Prod.*, 2014, **76**, p 180–189
16. J. Sharma and B.S. Sidhu, Investigation of Effects of Dry and Near Dry Machining on AISI D2 Steel Using Vegetable Oil, *J. Clean. Prod.*, 2014, **66**, p 619–623
17. S. Chincharikar and S.K. Choudhury, Hard Turning Using HiPIMS-Coated Carbide Tools: Wear Behavior Under Dry and Minimum Quantity Lubrication (MQL), *Measurement*, 2014, **55**, p 536–548
18. R.W. Maruda, S. Legutko, G.M. Krolczyk, and P. Raos, Influence of Cooling Conditions on the Machining Process Under MQCL and MQL Conditions, *The VJESN*, 2015, **22**(4), p 965–970
19. F. Klocke and G. Eisenblatter, Dry Cutting, *CIRP Ann. Manuf. Tech.*, 1997, **46**(2), p 519–526
20. R.W. Maruda, G.M. Krolczyk, E. Feldshtein, F. Pusavec, M. Szydłowski, S. Legutko, and A. Sobczak-Kupiec, A Study on Droplets Sizes, Their Distribution and Heat Exchange for Minimum Quantity Cooling Lubrication (MQCL), *Int. J. Mach. Tools Manuf.*, 2016, **100**, p 81–92
21. A.K. Rozentsvaig and ChS Strashinskii, Modeling of Heat Transfer Conditions in Cooling Lubricant Emulsions with Low-Boiling Continuous Media in Narrow Gaps, *Int. J. Heat Mass Trans.*, 2016, **102**, p 555–560
22. G. Krolczyk, P. Nieslony, and S. Legutko, Microhardness and Surface Integrity in Turning Process of Duplex Stainless Steel (DSS) for Different Cutting Conditions, *J. Mater. Eng. Perform.*, 2014, **23**(3), p 859–866
23. H. Hassanpour, M.H. Sadeghi, A. Rasti, and S. Shajari, Investigation of Surface Roughness, Microhardness and White Layer Thickness in Hard Milling of AISI 4340 Using Minimum Quantity Lubrication, *J. Clean. Prod.*, 2016, **120**, p 124–134
24. K. Gao, X. Qin, Z. Wang, and S. Zhu, Effect of Spot Continual Induction Hardening on the Microstructure of Steels: Comparison Between AISI 1045 and 5140 Steels, *Mater. Sci. Eng. A*, 2016, **651**, p 535–547
25. C.L. Pu, G. Zhu, S.B. Yang, E.B. Yue, and S.V. Subramanian, Effect of Dynamic Recrystallization at Tool-Chip Interface on Accelerating Tool Wear During High-Speed Cutting of AISI1045 Steel, *Int. J. Mach. Tools Manuf.*, 2016, **100**, p 72–80
26. C. Duan, W. Kong, Q. Hao, and F. Zhou, Modelling of White Layer Thickness in High Speed Machining of Hardened Steel Based on Phase Transformation Mechanism, *Int. J. Adv. Manuf. Technol.*, 2013, **69**, p 59–70
27. M. Rosiak, The Results of Consolidation of Sinters Being Deformed Under Complex Loading Condition, *Arch. Metall. Mater.*, 2013, **58**(4), p 1197–1206